SEMARAK ILMU PUBLISHING

Journal of Advanced Research in Fluid Mechanics and Thermal Sciences

Journal homepage:
https://semarakilmu.com.my/journals/index.php/fluid_mechanics_thermal_sciences/index
ISSN: 2289-7879

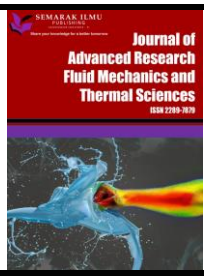

Analysis of Sound Propagation Behaviors for Supersonic Jet on Far Field Region by Computational Aero-Acoustics (CAA) Simulation

Yudi Maulana[1,2], Bukhari Manshoor[1,*], Amir Khalid[1], Izzuddin Zaman[1], Djamal Hissein Didane[1], Reazul Haq Abdul Haq[1], Kamarul-Azhar Kamarudin[1], Syahreen Nurmutia[2], Abdul Rafeq Saleman[3], Rio Marco Rathje[4], Christin Rothe[4], Mohd Nizam Ibrahim[5]

[1] Faculty of Mechanical and Manufacturing Engineering, Universiti Tun Hussein Onn Malaysia, Batu Pahat, Johor, Malaysia
[2] Fakultas Teknik and MIPA, Universitas Pamulang, Tangerang Selatan, Banten, Indonesia
[3] Faculty of Mechanical Engineering, Universiti Teknikal Malaysia Melaka, Durian Tunggal, Melaka, Malaysia
[4] Institute for Regenerative Energy Technology (in.RET), Nordhausen University of Applied Sciences, Nordhausen, Germany
[5] Maxpirations (M) Sdn Bhd, Sura Gate Commercial Centre, Dungun, Terengganu, Malaysia

ARTICLE INFO

Article history:
Received 11 November 2023
Received in revised form 8 April 2024
Accepted 19 April 2024
Available online 15 May 2024

Keywords:
Computational aeroacoustics; computational fluid dynamics; supersonic jet; sound propagation

ABSTRACT

Noise emission is an essential issue for the aviation industry, as it harms health and induces various physiological responses. The noise generated by supersonic jets is very intense. It will cause fatigue and even damage the human hearing system in the surrounding area of jet operation. Besides, the experimental and prototyping cost for the jet model is prohibitive, and it is a vast project and process that takes a lot of time to run. The purpose of this study is to determine the sound propagation behaviours of a supersonic jet in the far-field region and to analyse the consequences of the velocity of a supersonic jet on sound propagation of supersonic jet by using computational fluid dynamics (CFD) and computational aeroacoustics (CAA) simulations. This study focused on the perspective of observing the distance of the receiver when receiving the sound propagation of a supersonic jet, the observed angle of the receiver when receiving the sound propagation of a supersonic jet, and the velocity of the supersonic jet. The CFD and CAA analyses were performed in transient state simulation and the 2-inch Acoustics Reference Nozzle (ARN2). The result shows that the overall SPL throughout the frequency is proportional to the jet velocity of the supersonic jet. However, the distance and angle of the receiver gave different results in sound propagation behaviour. The results also conclude that as the distance between the receiver and jet nozzle exit increases, the overall SPL trend will decrease throughout the frequency increase. As the vertical distance between the receiver and the axisymmetric line of the jet nozzle increases, the frequency of the receiver starts to observe will decrease.

1. Introduction

Aeroacoustics is a branch of acoustics that studies the noise generated by aerodynamic motion such as turbulent fluid motion or interaction between solid surfaces [1-3]. One of the examples of

* *Corresponding author.*
E-mail address: bukhari@uthm.edu.my

https://doi.org/10.37934/arfmts.117.1.7182

aeroacoustics studies is the analysis of the noise propagation of a supersonic jet, which is a complicated source of acoustics radiation. Noise emission can be considered an essential issue for the aviation industry, especially in the neighbouring areas of airports when the aircraft is landing [4-6]. Noise exposure will have tremendous consequences on health and induce physiological responses such as increased heart rate, breathing and blood pressure [7-9]. The noise generated by supersonic jets is very intense. It will cause fatigue and even damage to the hearing system in the vicinity of the area where the supersonic jet is operating.

Supersonic jet noise consists of three major mechanisms: turbulent mixing noise, broadband shock-associated noise (BBSAN), and screech tone [10,11]. The turbulent mixing noise of the supersonic jet is contributed by two distinct components for jet flow, which are large turbulence structures and fine-scale turbulence. The large turbulent structures of the jet flow are quasi-coherent and quasi-orderly propagated and dominating at the downstream region beginning from the jet exit with tremendous speed relative to ambient sound speed, which means the minimum Mach number should be achieved by 1.0 [12-14]. The fine-scale turbulence of supersonic jet flow is radiated omnidirectionally and propagated mainly in the upstream and side-line regions. Overall, the sizeable turbulent structure noise will be more dominant than fine-scale turbulence in turbulent mixing noise for the supersonic jet flow [15-17]. Since the experimental and prototyping cost for the jet model is prohibitive and requires a lot of time to run the experiment, simulation-based methods such as computational aeroacoustics (CAA) and computational fluid dynamics (CFD) were proposed. Hence, this study aims to identify the sound propagation behaviour of a supersonic jet in a far-field region and analyse the consequences of the velocity of the supersonic jet using CFD and CAA simulation.

2. Previous Work

2.1 Noise Component

BBSAN is one of the main noise components of the supersonic jet when operating at off-design conditions, where the nozzle exit pressure is inequivalent to ambient pressure [18]. The disproportion of the shock system emerges and propagates in the jet plume and causes shock-associated noise, which is the interaction between the large turbulent structures and shock cell system, which is observed as an intense spectral peak associated with a lower strength of multiple peaks on downstream axis at relatively large angles to the jet [19,20]. In the situation of a heated jet, BBSAN and turbulent mixing noise are propagated frequently with the same intensity but in opposite directions. Thus, turbulent mixing noise is dominant at the downstream arc of the jet, while BBSAN is dominant at the upstream arc of the jet, but only in the case of peak sound levels. In low-frequency situations, the turbulent mixing noise will dominate all angles of the jet's axis due to the spectra of BBSAN decay quickly at low frequencies [21].

Screech tone is one of the components substituted by shock-associated noise, produced by a feedback loop. The feedback loop involves two elements, which are the flow disturbances inside the jet and feedback acoustic waves outside the jet. The flow disturbances inside the jet radiated downstream starting from the nozzle exit and undergo interaction with the shock cell structures, causing the noise to propagate upstream outside the supersonic flow and generating another disturbance that intersects with nozzle lips [22,23]. In this way, the resonant loop is created, which results in a screeching tone and associated harmonics. The screech tone will propagate essentially in the upstream direction of the jet, and it found that the first harmonic is most prominent in the normal direction of the jet centrelines.

2.2 Factor Influencing of Noise Propagation

Several parameters or variables will influence the noise propagation pattern of a supersonic jet, such as jet velocity, jet nozzle geometry, jet operating temperature, nozzle pressure ratio of the jet and so on. This study would mainly focus on the consequences of supersonic jet velocity towards noise propagation behaviour. Towne *et al.,* [24] studied the trapped wave properties at the boundary of different Mach number regimes (*M* =0.4, 0.7, 0.8, 0.9 and 1.5) using large eddy simulation. From their works, they found that in the range of Mach numbers from 0.82 to 1.0, the resonance between the pair of tubular modes predicted by the vortex sheet model persists to lower Mach numbers and is gradually damped. However, the resonance is unavailable at Mach number, which is higher than 1.0. Instead, the weaker interaction between a different pair of trapped waves is observed.

Besides, to understand the consequences of the Mach number and Reynolds number of a supersonic jet, Bellan [25] experimented by operating a supersonic jet at Reynold numbers (Re = 1500, 3700, 7900) with Mach numbers (M_a =1.4, 2.1) and simulated via large-eddy simulation. They found that the potential core of a jet with a smaller Mach number is shorter, and its length is unrelated to the Reynolds number. The M_a =1.4 jet propagate further in the lateral direction than M_a =2.1 jet due to the earlier transition to turbulence (shorter potential kernel) at lower Mach numbers. At a given axial position, the centreline turbulence of the high Mach number jets is more intense; however, high Mach number jets decay faster along the radial direction as the delayed transition of M_a =2.1 jets, which results in a smaller spread of the jet at a given axial position.

Moreover, Li and Gao [26] investigated the screech phenomenon of the supersonic jet Mach numbers (M_a) in the range of 1.17 to 1.60. They compared the numerical result with the experimental result from previous research, which showed a good agreement. They found that the simulated wavelengths consist of both flapping (B mode) and helical oscillation modes (C mode) simultaneously in the Mach number ranging from 1.38 to 1.41. From the numerical data obtained, it can be observed that the dominance oscillation mode will be shifted from B mode to C mode when it occurs at approximately M_a =1.40. This research shows that the Mach number is one of the elements that will affect the screech phenomenon of jet flow when operating with different Mach numbers.

3. Methodology

In this research, ANSYS Fluent software w$|M_\infty|$as used to perform numerical simulations. The performance and acoustic behaviours of supersonic jets in far-field regions were observed. The noise propagation of the supersonic jet on the far-field region will be analysed in CAA associated with the Ffowcs Williams-Hawkings (FW-H) solver [27]. The FW-H equation, as the general form of the Lighthill acoustic analogy is an exact rearrangement of the continuity and Navier-Stokes equations used for calculating noise propagated from arbitrarily moving bodies.

$$\left\{\frac{1}{c_0^2}\frac{\partial^2}{\partial t^2}-\frac{\partial^2}{\partial x^2}\right\}\left[p'(\boldsymbol{x},t)H(f)\right]=\frac{\partial}{\partial t}\left[L_i\delta(f)\right]+\frac{\partial^2}{\partial x_i\partial x_j}\left[T_{ij}H(f)\right] \tag{1}$$

The classical FW-H equation interprets sound as a response of an inhomogeneous wave equation in a medium at rest. When one considers the effects of mean flow (for $|M_\infty|$<1), the free-space Green's function for the two-dimensional FW-H equation can be expressed as:

$$G(\boldsymbol{x},t;\boldsymbol{y},\tau)=\frac{i\lambda}{8\pi}\int_{-\infty}^{\infty}e^{-ik\lambda^2\gamma M_\infty}H_0^{(1)}\left(k\lambda^2R^*\right)e^{-i\omega(t-\tau)}d\omega \tag{2}$$

In Eq. (2), $H_0^{(1)}$ is the zero-order Hankel function of the first kind and $i=\sqrt{-1}.k=\omega/c_0$ is the acoustic wave number, whereas ω is the angular frequency. Since noise prediction is usually required in the far-field, we can use a far-field simplification. As the approximations are realized by a Taylor expansion around $\eta=1$ and $t=0$, the origin must be defined near the data curve and the observer be located far from the sources. Thus, $|\eta|$ is required to be small or at least on the order of the spatial extension of the data line, i.e. $|x|\square\ |\eta|$ and $kr\square\ 1$.

3.1 Geometry Modelling

For the model geometry of the present investigation, the supersonic jet nozzle model was Acoustic Reference Nozzle (ARN2) developed using SolidWorks software. Since this study is a 2-dimensional problem, the jet model was developed as a 2-D model. The diameter of the jet nozzle exit is 5.08 cm (2 inches), and it is a conical convergent nozzle with a converging angle of 30°. Figure 1 shows the jet operation geometry. After the ARN2 jet nozzle model was developed, the model was imported to the ANSYS DesignModeler software to create the jet operation geometry. Figure 2 shows the model geometry of axisymmetric ARN 2 jet nozzles, while Figure 3 shows the atmosphere of the jet operation geometry with a 1000 m diameter to simulate the actual condition when the supersonic jet was operated. The jet operation geometry was located in the middle of the atmosphere and above the axis line of the atmosphere.

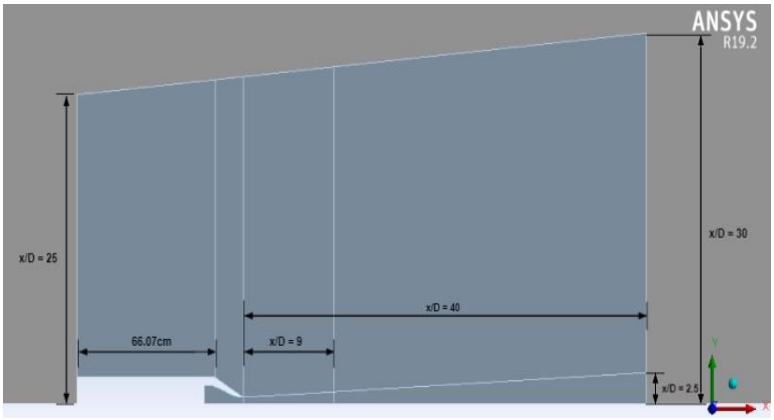

Fig. 1. Jet operation model

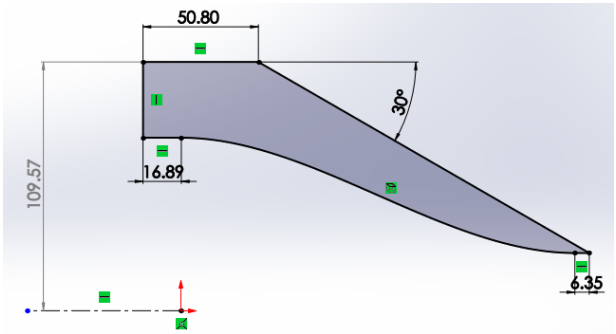

Fig. 2. Model geometry of ARN2 jet nozzle (Dimension in mm units)

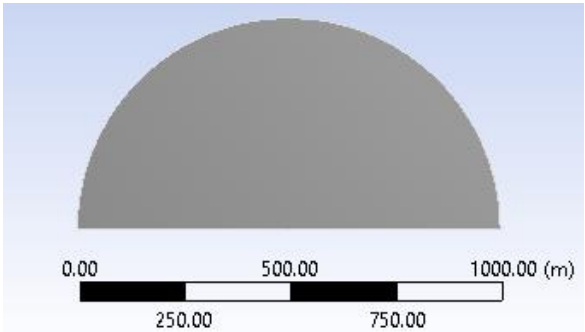

Fig. 3. Atmospheric of jet operation geometry

3.2 Meshing and Boundary Conditions

Meshing is a process in which it refines to smaller cells for obtaining high solution gradients and fine geometric detail. The meshing process was conducted using several division methods to the edge of geometries. The mesh shape of the jet operation geometry was presented in quadrilateral form while the mesh shape of the atmosphere would be presented in triangle form. Figure 4(a) shows the grid for jet operation geometry while Figure 4(b) shows the atmosphere grid after finishing the meshing process.

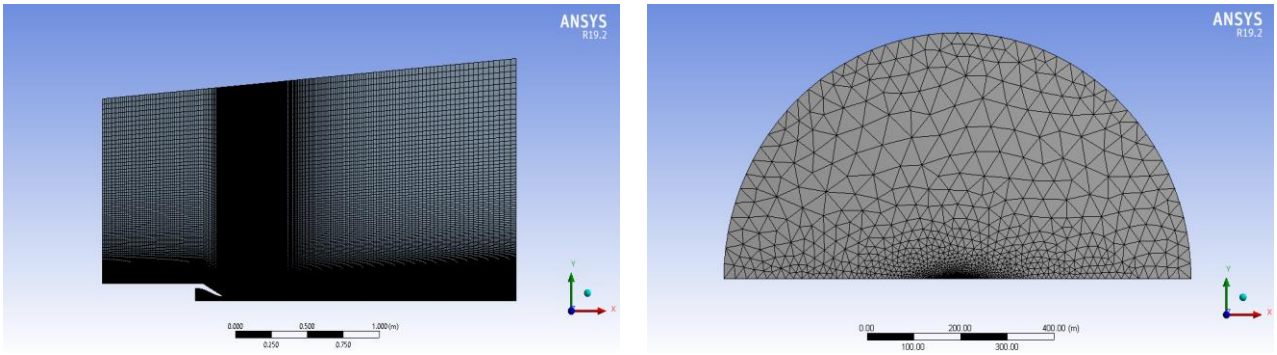

(a) (b)

Fig. 4. (a) Jet operation geometry grid, (b) Atmosphere grid

Grid Independent Test (GIT) was performed to ensure a precise and valid result in the CFD processor by perpetuating the GIT as low as possible without disturbing the result. This step proceeded before the verification process. Table 1 shows the result of the comparison of relative error, while Figure 5 shows the graph of GIT, which plotted the jet operation velocity for different modes of mesh against the position of the jet operation grid. As a result, the mode D grid was chosen as the grid for this study since the relative error of mode D is lower compared to mode C and mode E. Besides, the final jet operation velocities of mode D and mode E are approximately the same. However, the computational cost of mode D is lower than that of mode E.

Table 1
Comparison of Relative Error

Mode	Number of Nodes	Number of Elements	Maximum Skewness	Min. Orthogonal Quality	Average Velocity (m/s)	Relative Error (%)
A	14426	15360	0.45061	0.57413	251.8886	-
B	51081	51735	0.36384	0.74069	253.6828	0.7123
C	111486	111860	0.33333	0.76673	257.6310	1.5564
D	197651	197735	0.33333	0.79953	260.2362	1.0112
E	328956	328735	0.33333	0.82103	254.1956	2.3212

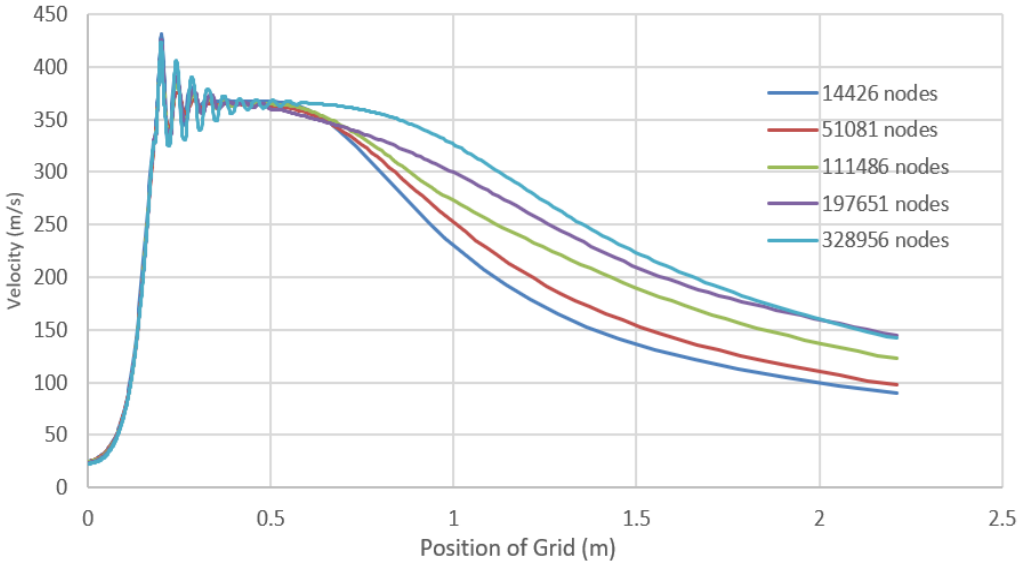

Fig. 5. Grid-independent test

Boundary condition plays a significant role in ANSYS Fluent as it assists the fluid flow in noticing where the system is limited. This study consisted of several boundary conditions, which are inlet boundary condition, outlet boundary condition, wall condition and axisymmetric boundary condition, which are shown in Figure 6. The supersonic jet is operated in a total temperature ratio (TTR) of 1.0. For the pressure inlet, the total gauge pressure was predicted by using the equation as shown in Eq. (3). For the pressure outlet, the gauge pressure was set at 100000 Pa. As for the nozzle wall, the specified shear was set, and all the values were set as 0.

$$\frac{P}{P_t} = \left(1 + \frac{\gamma - 1}{2} M_j^2\right)^{-\frac{\gamma}{\gamma - 1}} \tag{3}$$

P is the pressure-inlet transformed from jet velocity, P_t is the pressure of whole conditions, which is 100000 Pa, γ is the specific heat ratio, which is 1.4 (isentropic flow) and M_j is the Mach number of the supersonic jet.

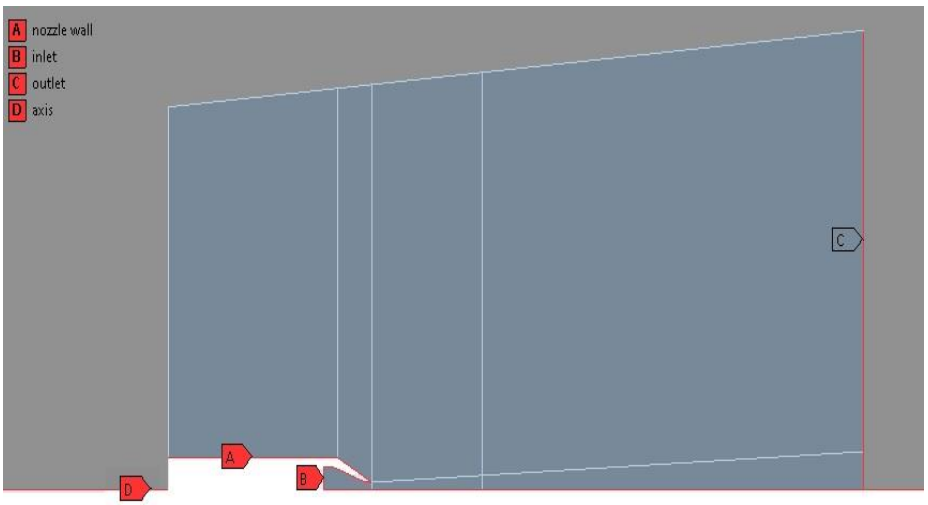

Fig. 6. Boundary condition of jet operation geometry

3.3 Method of Solution

In the present research, Computational Fluid Dynamics (CFD) and Computational Aeroacoustics (CAA) will be utilized and simulated via ANSYS Fluent software. The turbulent flow of the supersonic jet will be analysed in CFD associated with the Reynold-averaged Navier-Stoke (RANS) equation and realizable k-ε model. The noise propagation of a supersonic jet in the far-field region will be analysed in CAA associated with Ffowcs Williams-Hawkings (FW-H) solver.

4. Results and Discussion

For the verification process, the graphical data of a previous study authored by Seiner *et al.,* [28] were used to verify the simulation of this study. Figure 7 shows the graph of V/V_j against *X/D* which represents the comparison between experimental data and verification simulation data. The average value of the jet velocity ratio (V/V_j) for verification simulation data is 0.8796 while the average value of the jet velocity ratio (V/V_j) for journal experimental data is 0.9060. The relative error between both studies is 2.914% which is less than 10%.

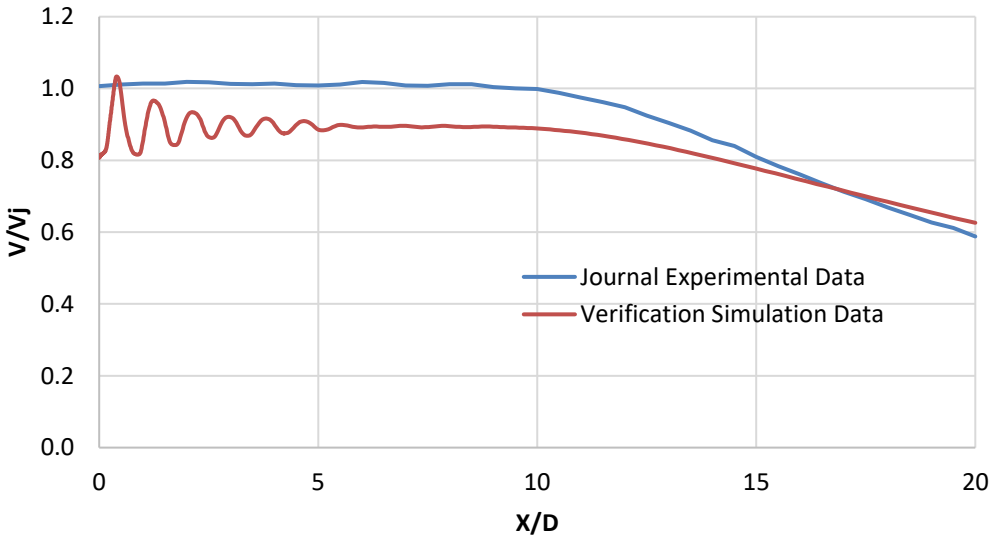

Fig. 7. Comparison between experiment and simulation data

4.1 Velocity Contour Analysis

Velocity contour is defined as an approach to measuring flow by profiling point velocities and converting them to average cross-sectional flow rates. These averages are later multiplied with the cross-section area to obtain the discharge. Figure 8 shows the velocity contour of a supersonic jet with a Mach number of 1.0 to 1.4. From Figure 8(a) to Figure 8(e), all the velocity contours of a supersonic jet, it was observed that the shock cells appeared near the jet nozzle exit, and the shock cells were getting more pronounced as they went down from Mach 1.0 to Mach 1.4 supersonic jet. The shock cells presented at the velocity contour of the Mach 1.4 supersonic jet were the most obvious, which presented the red crosses near the jet nozzle exit. Besides, it was observed the external velocity flows were spread out to the surrounding of the jet which presented in the velocity contour of a Mach 1.4 supersonic jet, which means the unsteady jet velocity flows began in Mach 1.4 supersonic jet as the jet velocity is highly huge.

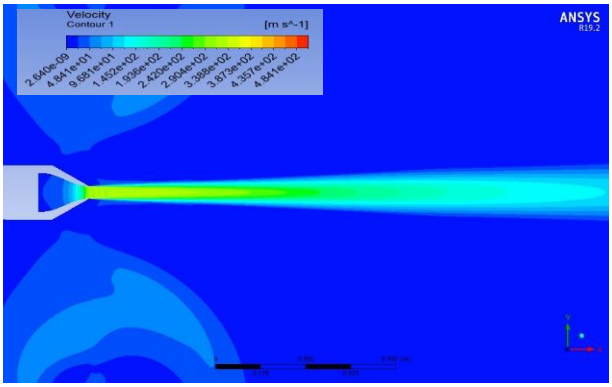

(a) Mach 1.0 Supersonic Jet

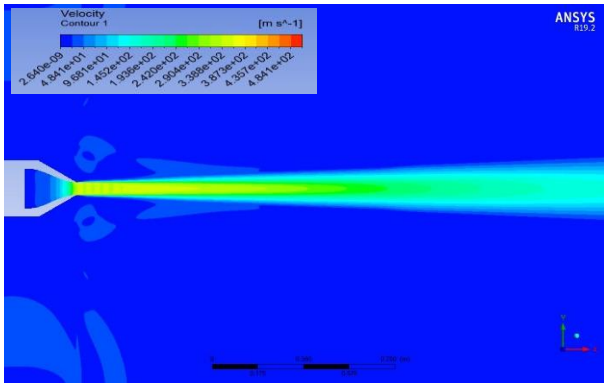

(b) Mach 1.1 Supersonic Jet

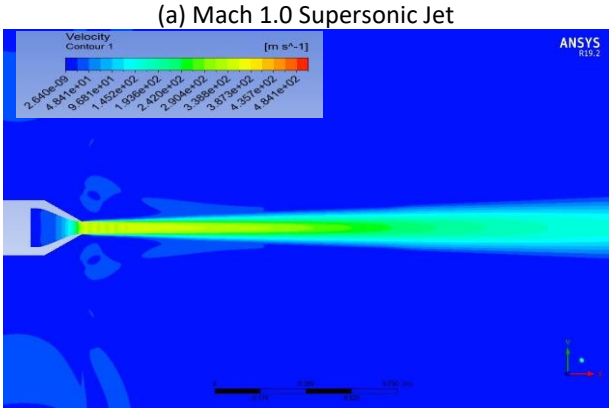

(c) Mach 1.2 Supersonic Jet

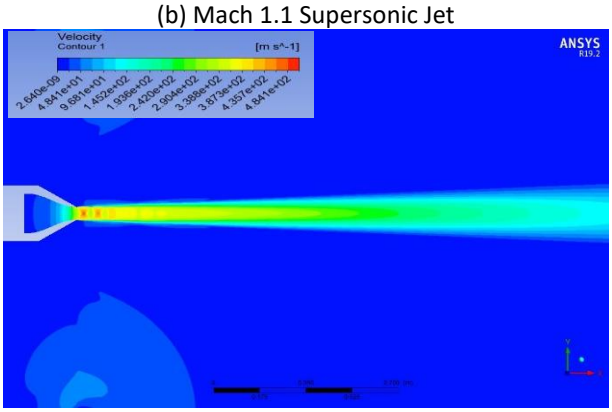

(d) Mach 1.3 Supersonic Jet

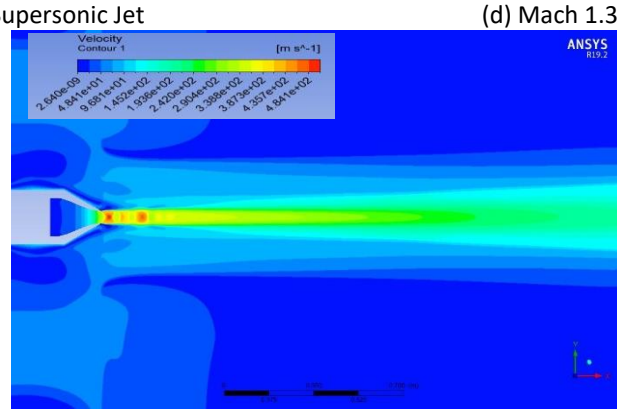

(e) Mach 1.4 Supersonic Jet

Fig. 8. Velocity contour of supersonic jet

4.2 Distance Effect on the Sound Propagation Behaviour

To observe the sound propagation behaviour of a supersonic jet with different observe distances, several receivers were applied in the simulation. The velocity of the supersonic jet remains constant, which is M_j = 1.2. The observed angle of the receivers is constant, which is 30° upwards from the axisymmetric line of the jet nozzle. The different observed distances of the receivers from the jet nozzle exit are x/D = 10, x/D = 20 and x/D = 40, whereas the jet nozzle exit was set as an origin (0,0). Figure 9 shows the graphical result of sound propagation behaviour obtained in all receivers. It was observed that the receiver x/D = 10 was starting to observe sound pressure level (SPL) at a lower frequency compared to the receiver x/D = 20 and x/D = 40. The amplitude SPL of receiver 3 was the highest compared to the receiver x/D = 10 and x/D = 20. From the frequency of 100 kHz, the SPL of the receiver x/D = 40 was the highest compared to the receiver x/D = 10 and x/D = 20. The SPL of all receivers is similar in the range of around 2000 Hz to 5500 Hz. This can be concluded that as the observed distance between the receiver and jet nozzle exit increases, the overall SPL trend will be

decreased throughout the frequency increase. Besides, the observed distance between the receiver and jet nozzle exit increases, and the beginning observed frequency will be increased.

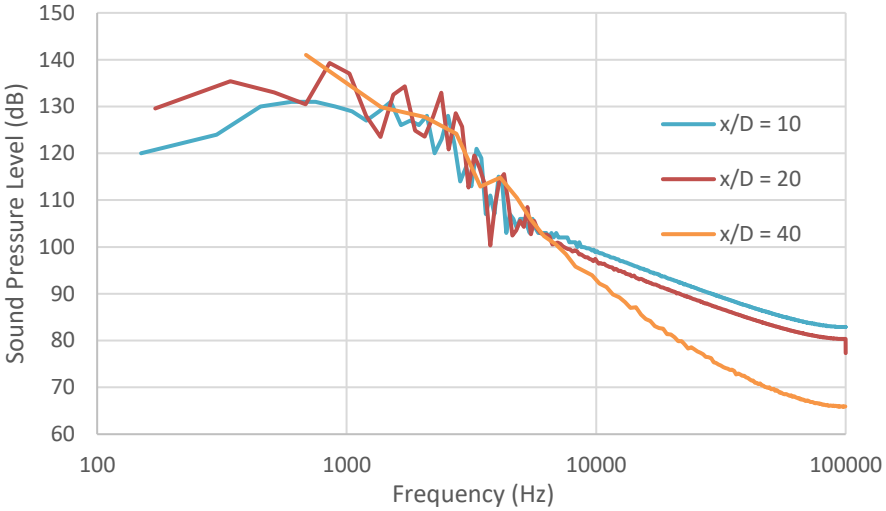

Fig. 9. Sound propagation of supersonic jet in different observed distances of the receiver

4.3 An Effect of Angle on Sound Propagation Behaviour

For determining the effect of sound propagation behaviour of a supersonic jet with different observation angles, several receivers were adopted in the simulation. The velocity of the supersonic jet remains constant, which is M_j = 1.2. The observed distance of the receivers is constant, which are located at x/D = ±10 from the jet nozzle exit which coordinated as (0,0). The different observed angles of the receivers are 30°, 60°, 80°, 120° and 150° upwards from the axisymmetric line of the jet nozzle. Figure 10 shows the graphical result of sound propagation behaviour obtained in all receivers. It was observed that the receiver at 30° was starting to observe SPL at a lower frequency compared to other receivers. The amplitude SPL of the receiver at 60° was the highest compared to other receivers which was 138 dB. From the frequency of 100 kHz, the SPL of the receiver at 80° was the highest compared to other receivers. This can be concluded that as the vertical distance between the receiver and the axisymmetric line of the jet nozzle increases the frequency of the receiver starts to observe will be decreased. Besides, the overall SPL observed at the backwards of the jet nozzle exit is lower compared to the forward of the jet nozzle exit.

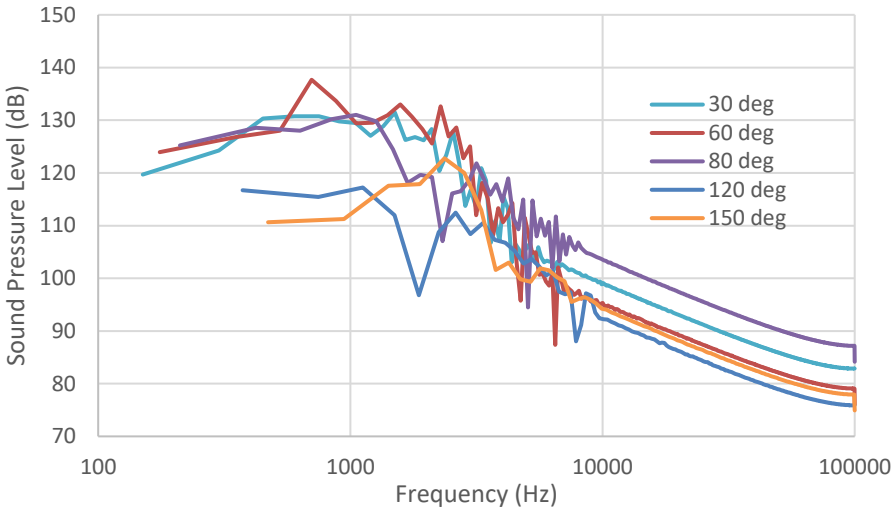

Fig. 10. Sound propagation of supersonic jet in different observed distances of angle

4.4 Velocity Effect on Sound Propagation Behaviour

For analysing the consequences of sound propagation behaviour of supersonic jets with different jet velocities, which are Mach number (M_a = 1.0, 1.1, 1.2, 1.3 and 1.4). The observed distance and angle of the receivers remain unchanged, located at x/D = 20 from the jet nozzle exit, which is coordinated as (0,0), 30° observed angle upwards from the axisymmetric line of the jet nozzle. Figure 11 shows the graphical result of sound propagation behaviour obtained in different jet velocities. It was observed that the overall trend of SPL data was similar when operated in different supersonic jet velocities since the observed location of the receiver was fixed. When the jet velocity of the supersonic jet increased, the overall SPL trend throughout the frequency also increased.

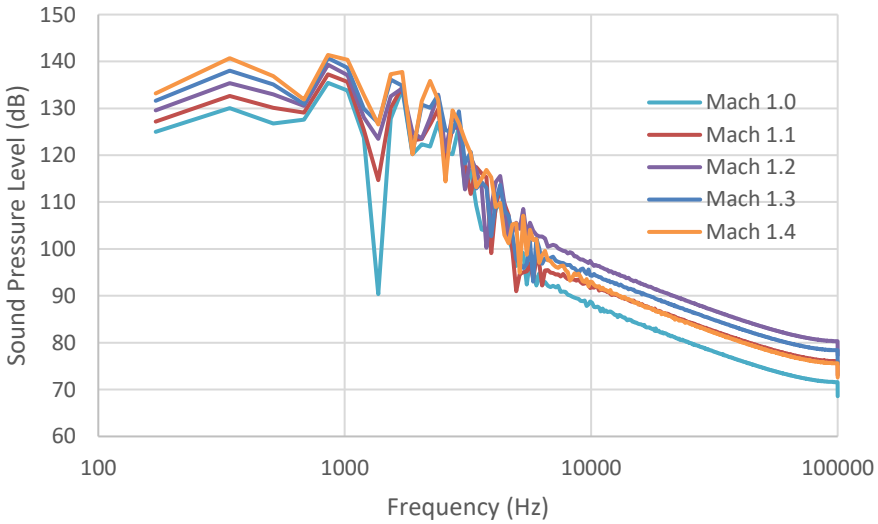

Fig. 11. Sound propagation of supersonic jet in different jet velocity

5. Conclusion

Throughout this study, the sound propagation behaviors of a supersonic jet on a far-field region were identified and the effects of the velocity of a supersonic jet on sound propagation of a

supersonic jet were analysed by using CFD and CAA simulations. When operating with different jet velocities, the overall sound propagation behaviour of the supersonic jet was similar. As the jet velocity of the supersonic jet increased, the overall SPL throughout the frequency also increased. Different observed distances and angles of the receiver will result in different sound propagation behaviour of the supersonic jet. As the observed distance between the receiver and jet nozzle exit increases, the overall SPL trend will decrease throughout the frequency increase. As the vertical distance between the receiver and the axisymmetric line of the jet nozzle increases, the frequency of the receiver starts to observe will decrease.

Acknowledgement

This research was supported by the Ministry of Higher Education (MOHE) through the Fundamental Research Grant Scheme (FRGS/1/2022/TK08/UTHM/02/14), Vot K434. We also want to thank the Universiti Tun Hussein Onn Malaysia via sabbatical leave scheme, the Institute for Regenerative Energy Technology (in.RET), Nordhausen University of Applied Sciences and Maxpirations (M) Sdn Bhd for supporting data and technical advice.

References

[1] Li, Xiao-dong, Min Jiang, Jun-hui Gao, Da-kai Lin, Li Liu, and Xiao-yan Li. "Recent advances of computational aeroacoustics." *Applied Mathematics and Mechanics* 36, no. 1 (2015): 131-140. https://doi.org/10.1007/s10483-015-1899-9

[2] Li, Siye, Yu Hu, Zhensheng Sun, YiAng Shi, and Kai Mao. "A high-resolution finite volume scheme based on optimal spectral properties of the fully discrete scheme with minimized dispersion and adaptive dissipation." *Computers & Fluids* 233 (2022): 105226. https://doi.org/10.1016/j.compfluid.2021.105226

[3] Tam, Christopher K. W. "Recent advances in computational aeroacoustics." *Fluid Dynamics Research* 38, no. 9 (2006): 591. https://doi.org/10.1016/j.fluiddyn.2006.03.006

[4] Mancinelli, Matteo, Vincent Jaunet, Peter Jordan, Aaron Towne, and Stève Girard. "Reflection coefficients and screech-tone prediction in supersonic jets." In *25th AIAA/CEAS Aeroacoustics Conference*, p. 2522. 2019. https://doi.org/10.2514/6.2019-2522

[5] Edgington-Mitchell, Daniel, Vincent Jaunet, Peter Jordan, Aaron Towne, Julio Soria, and Damon Honnery. "Upstream-travelling acoustic jet modes as a closure mechanism for screech." *Journal of Fluid Mechanics* 855 (2018): R1. https://doi.org/10.1017/jfm.2018.642

[6] Mancinelli, Matteo, Tiziano Pagliaroli, Roberto Camussi, and Thomas Castelain. "On the hydrodynamic and acoustic nature of pressure proper orthogonal decomposition modes in the near field of a compressible jet." *Journal of Fluid Mechanics* 836 (2018): 998-1008. https://doi.org/10.1017/jfm.2017.839

[7] Manshoor, Bukhari, and Amir Khalid. "Numerical investigation of the circle grids fractal flow conditioner for orifice plate flowmeters." *Applied Mechanics and Materials* 229 (2012): 700-704. https://doi.org/10.4028/www.scientific.net/AMM.229-231.700

[8] Méline, Julie, Andraea Van Hulst, Frédérique Thomas, Noëlla Karusisi, and Basile Chaix. "Transportation noise and annoyance related to road traffic in the French RECORD study." *International Journal of Health Geographics* 12 (2013): 1-13. https://doi.org/10.1186/1476-072X-12-44

[9] Jacyna, Marianna, Mariusz Wasiak, Konrad Lewczuk, and Grzegorz Karoń. "Noise and environmental pollution from transport: decisive problems in developing ecologically efficient transport systems." *Journal of Vibroengineering* 19, no. 7 (2017): 5639-5655. https://doi.org/10.21595/jve.2017.19371

[10] Tam, Christopher K. W. "Supersonic jet noise." *Annual Review of Fluid Mechanics* 27, no. 1 (1995): 17-43. https://doi.org/10.1146/annurev.fluid.27.1.17

[11] Manshoor, Bukhari, Chia I. Shin, Djamal Hissein Didane, Amir Khalid, and Muhammed Abdelfattah Sayed Abdelaal. "Numerical Study on Aeroacoustics Behaviour of Contra-Rotating Fans." *International Journal of Engineering Trends and Technology* 69, no. 8 (2021): 109-116. https://doi.org/10.14445/22315381/IJETT-V69I8P214

[12] Tam, Christopher K. W., K. Viswanathan, K. K. Ahuja, and J. Panda. "The sources of jet noise: experimental evidence." *Journal of Fluid Mechanics* 615 (2008): 253-292. https://doi.org/10.1017/S0022112008003704

[13] Liu, Xiran, Dan Zhao, Di Guan, Sid Becker, Dakun Sun, and Xiaofeng Sun. "Development and progress in aeroacoustic noise reduction on turbofan aeroengines." *Progress in Aerospace Sciences* 130 (2022): 100796. https://doi.org/10.1016/j.paerosci.2021.100796

[14] Sadeghian, Mojtaba, and Mofid Gorji Bandpy. "Technologies for Aircraft Noise Reduction: A Review." *Journal of Aeronautics & Aerospace Engineering* 9, no. 1 (2020).
[15] Bai, Baohong, Xiaodong Li, and Haixin Chen. "A Semi-empirical Prediction Method for the Fine Scale Turbulence Mixing Noise." In *25th AIAA/CEAS Aeroacoustics Conference*, p. 2757. 2019. https://doi.org/10.2514/6.2019-2757
[16] Morris, Philip J., and F. Farassat. "Acoustic analogy and alternative theories for jet noise prediction." *AIAA Journal* 40, no. 4 (2002): 671-680. https://doi.org/10.2514/2.1699
[17] Zaman, Izzuddin Bin, Muhammad Mohamed Salleh, Bukhari Manshoor, Amir Khalid, and Sherif Araby. "The application of multiple vibration neutralizers for vibration control in aircraft." *Applied Mechanics and Materials* 629 (2014): 191-196. https://doi.org/10.4028/www.scientific.net/AMM.629.191
[18] Kalyan, Anuroopa, and Sergey A. Karabasov. "Broad band shock associated noise predictions in axisymmetric and asymmetric jets using an improved turbulence scale model." *Journal of Sound and Vibration* 394 (2017): 392-417. https://doi.org/10.1016/j.jsv.2017.01.027
[19] André, Benoît, Thomas Castelain, and Christophe Bailly. "Broadband shock-associated noise in screeching and non-screeching underexpanded supersonic jets." *AIAA Journal* 51, no. 3 (2013): 665-673. https://doi.org/10.2514/1.J052058
[20] Powell, Alan, Yoshikuni Umeda, and Ryuji Ishii. "Observations of the oscillation modes of choked circular jets." *The Journal of the Acoustical Society of America* 92, no. 5 (1992): 2823-2836. https://doi.org/10.1121/1.404398
[21] Morris, Philip, and Steven Miller. "The prediction of broadband shock-associated noise using RANS CFD." In *15th AIAA/CEAS Aeroacoustics Conference (30th AIAA Aeroacoustics Conference)*, p. 3315. 2009. https://doi.org/10.2514/6.2009-3315
[22] Tam, Christopher K. W., Sarah A. Parrish, and Krishna Viswanathan. "Harmonics of jet screech tones." *AIAA Journal* 52, no. 11 (2014): 2471-2479. https://doi.org/10.2514/1.J052850
[23] Shen, Hao, and Christopher K. W. Tam. "Effects of jet temperature and nozzle-lip thickness on screech tones." *AIAA Journal* 38, no. 5 (2000): 762-767. https://doi.org/10.2514/2.1055
[24] Towne, Aaron, Oliver T. Schmidt, and Guillaume A. Bres. "An investigation of the Mach number dependence of trapped acoustic waves in turbulent jets." In *25th AIAA/CEAS Aeroacoustics Conference*, p. 2546. 2019. https://doi.org/10.2514/6.2019-2546
[25] Bellan, Josette. "Large-eddy simulation of supersonic round jets: effects of Reynolds and Mach numbers." *AIAA Journal* 54, no. 5 (2016): 1482-1498. https://doi.org/10.2514/1.J054548
[26] Li, X. D., and J. H. Gao. "Numerical simulation of the three-dimensional screech phenomenon from a circular jet." *Physics of Fluids* 20, no. 3 (2008). https://doi.org/10.1063/1.2844474
[27] Wang, Xiao, Shanti Bhushan, Bukhari Manshoor, Edward A. Luke, Adrian Sescu, Yuji Hattori, David S. Thompson, and Keith Walters. "Dynamic Hybrid RANS/LES Assessment of Sound Generation and Propagation for Flow Over a Circular Cylinder." In *2018 AIAA/CEAS Aeroacoustics Conference*, p. 3592. 2018. https://doi.org/10.2514/6.2018-3592
[28] Seiner, John M., Michael K. Ponton, Bernard J. Jansen, and Nicholas T. Lagen. "The effects of temperature on supersonic jet noise emission." In *14th DGLR/AIAA Aeroacoustics Conference*, vol. 1, pp. 295-307. 1992.